

Accepted manuscript doi: 10.1680/jgeot.16.p.281

Accepted manuscript

As a service to our authors and readers, we are putting peer-reviewed accepted manuscripts (AM) online, in the Ahead of Print section of each journal web page, shortly after acceptance.

Disclaimer

The AM is yet to be copyedited and formatted in journal house style but can still be read and referenced by quoting its unique reference number, the digital object identifier (DOI). Once the AM has been typeset, an 'uncorrected proof' PDF will replace the 'accepted manuscript' PDF. These formatted articles may still be corrected by the authors. During the Production process, errors may be discovered which could affect the content, and all legal disclaimers that apply to the journal relate to these versions also.

Version of record

The final edited article will be published in PDF and HTML and will contain all author corrections and is considered the version of record. Authors wishing to reference an article published Ahead of Print should quote its DOI. When an issue becomes available, queuing Ahead of Print articles will move to that issue's Table of Contents. When the article is published in a journal issue, the full reference should be cited in addition to the DOI.

Accepted manuscript doi: 10.1680/jgeot.16.p.281

Submitted: 02 November 2016

Published online in 'accepted manuscript' format: 19 December 2017

Manuscript title: Suction caissons in dense sand, Part I: Installation, limiting capacity and drainage

Authors: B. Bienen*, R. T. Klinkvort[†], C. O'Loughlin*, F. Zhu* and B. W. Byrne[‡]

Affiliations: *Centre for Offshore Foundation Systems, The University of Western Australia, 35 Stirling Hwy, Crawley, Perth, WA 6009, Australia; [†]Norwegian Geotechnical Institute, Sognsveine 72, Oslo 0855, Norway and [‡]Department of Engineering Science, The University of Oxford, Parks Road, Oxford, OX1 3PJ, UK

Corresponding author: B. Bienen, Centre for Offshore Foundation Systems, The University of Western Australia, 35 Stirling Hwy, Crawley, Perth, WA 6009, Australia. Tel: +61 (0) 8 6488 4246.

E-mail: britta.bienen@uwa.edu.au

Abstract

Suction caissons are a promising foundation concept for supporting offshore wind turbines. Compared to applications in the oil and gas industry, where most practical experience exists, significant differences arise in terms of load paths and magnitudes, soil type and caisson aspect ratio (skirt length to diameter). In a set of two companion papers, this contribution investigates the response of suction caissons in dense sand through a series of centrifuge experiments. The caisson was installed using suction, followed by sequences of cyclic loading and then extraction, all steps completed continuously in-flight. This first paper discusses installation, limiting capacities and drainage, whereas the second paper focuses on vertical cyclic loading into tension. The work demonstrates that suction caisson installation behaviour is well described by existing calculation methods. Tests performed at different installation rates demonstrate that careful assessment of the pumping rate is needed to ensure successful installation, with low pumping rates resulting in premature refusal. In the centrifuge tests, full skirt penetration was achieved without apparent loosening of the soil plug. The limiting capacity in tension, measured during the testing at both fast and slow uplift rates, was also well described by existing calculation methods.

Key words: Suction; footing/foundation; offshore engineering; centrifuge modelling; sand

INTRODUCTION

A foundation concept that is gaining acceptance for the support of bottom-fixed offshore wind turbines (OWTs) is the suction caisson. This may support the turbine superstructure either as an individual caisson or as a group of three or four caissons below a jacket substructure, as shown in Figure 1. A suction caisson is composed of a cylinder that is open at the base and closed at the top. During installation the foundation is lowered to the seabed, with the skirts penetrating the soil, until sufficient bearing capacity is mobilised to support the self-weight. During this phase water is allowed to escape through open valves in the lid. Once the self-weight skirt penetration has completed, sufficient to create a seal between the skirt and soil, water is evacuated from within the caisson by means of a pumping system. The differential pressure (suction) created across the caisson lid drives the caisson into the seabed. In sand, the seepage flow that develops around the caisson skirt reduces the effective stresses at the skirt tip (Houlsby and Byrne, 2005; Andersen et al., 2008), which is essential for successful installation, particularly in dense sands. This process is shown schematically in Figure 2.

The design of an OWT differs from other more typical offshore installations in important ways. Strict rotational limits of 0.25° tilt are typically enforced (Peire et al., 2009) for serviceability. Foundation response is integral to the overall system behaviour, and any deformation at foundation level contributes to a net rotation of the OWT. Therefore deformation (i.e. load states that govern serviceability (SLS) and fatigue (FLS) response), rather than capacity (ultimate limit state ULS), is likely to be the critical design criterion for caisson foundations. Furthermore, OWTs are generally designed as soft-stiff systems, with a target eigenfrequency that falls in the narrow range between that of the single blade passing frequency (1P) and the rotor frequency (3P), where LeBlanc (2009) refers to typical ranges of frequencies $1P = 0.17\text{-}0.33$ Hz and $3P = 0.5\text{-}1.0$ Hz. The system eigenfrequency is influenced significantly by the foundation stiffness, which depends on the soil state, the loads transferred to the foundation, drainage conditions and other factors. The stiffness of response may change over the design life of the OWT. Kallehave et al. (2015) report an eigenfrequency between 0.345 and 0.365 Hz from in-situ measurements on monopiles, with the eigenfrequency apparently decreasing during storm loading. Due to different load paths and

soil nonlinearity, the stiffness may also differ between the individual foundations of a multi-footing structure.

Suction caissons have been used successfully for decades in the oil and gas industry (Eide and Andersen, 1984; Tjelta et al., 1986; Hansen et al., 1992; Bye et al., 1995; Andersen et al., 2005). By comparison with the OWT such structures are typically much heavier and experience comparatively smaller horizontal and moment loads from the wind and wave action. They are also normally a one-off installation in which the foundation design may not be the critical element. In contrast, the wind farm may comprise of 100 to 300 OWTs across a large site with significant economies to be derived from better foundation design or alternative foundation concepts. However, practical experience using suction caissons at full scale for offshore renewable energy has been rather limited. A prototype mono-caisson was installed in Frederikshavn harbour, Denmark, in 2002, supporting a 3 MW wind turbine on dense sand (Ibsen, 2008). This installation is, however, sheltered from wave loading. There are recent instances of monitored suction caissons, used as mono-caissons, for met masts at Horns Rev 2 and Dogger Bank (Tjelta, 2015). In 2014 a monitored tripod structure, supporting a 4 MW turbine, was installed on suction caissons at Borkum Riffgrund (Tjelta, 2015). At the same time a large field campaign of suction caisson trial installations has been performed in the North Sea, through the Carbon Trust Wind Accelerator programme. The information from these activities will play an important role in informing design more widely, although most of the data currently remains confidential.

Calculation methods for the prediction of installation for suction caissons in sand are available, and have been shown to capture well the observed suction assisted installation response in the field and in the laboratory (Houlsby and Byrne, 2005; Andersen et al., 2008; Senders and Randolph, 2009). Different data sets require slightly different, but consistent parameter values, as would be expected (discussed further in Andersen et al., 2008). All methods allow prediction of self-weight penetration as well as the suction required for complete installation. Houlsby and Byrne (2005) also provide a simple calculation to assess required pumping rates taking account of the seepage flow. The potential effect of the pumping rate on the soil state, as a result of suction installation, is not discussed.

Research on the response of suction caissons in sand under cyclic loading has relied heavily on experiments, performed mostly on the laboratory floor at model scale but also at elevated accelerations in a geotechnical centrifuge and at medium scale in the field. Initial investigations addressed monotonic behaviour (Byrne, 2000) and transient loading reflecting extreme storm events (Byrne and Houlsby, 2002; 2004, Houlsby et al., 2005a). A change in foundation stiffness was observed as the loading moved from compressive to tensile. A significant conclusion from these studies was that design for tensile loading would be governed by serviceability requirements. Large tensile capacities could be achieved, limited by cavitation of the pore fluid, though these were normally accompanied by large displacements. The experimental database from single gravity small scale model tests (Zhu et al., 2013; Kelly et al., 2006b) and medium scale field tests (Houlsby et al., 2006; Kelly et al., 2006a) has been complemented by results from centrifuge modelling of a caisson, installed by suction at enhanced gravity, followed by monotonic or cyclic vertical (Senders, 2008) or lateral loading (Cox et al., 2014). The monotonic tests demonstrated an increase in resistance as the loading velocity was increased, consistent with the findings of Bye et al. (1995), Byrne and Houlsby (2002) and Houlsby et al. (2005a), and also consistent with the expected behaviour for dilatant soil. The cyclic test results are also consistent with previous work indicating that serviceability under tensile loading is critical.

Despite the significant research effort, the following questions remain, which are addressed in this set of papers:

- What is the effect of the pumping rate on caisson installation? The suction installation should ensure full skirt penetration (even in very dense sand) without significant loosening of the soil plug.
- What is the effect of the suction installation process on the subsequent foundation stiffness and deformation response under cyclic loading? This will provide insight into whether the OWT can meet the strict deformation limit criteria over the lifetime.
- What is the effect of load excursions into tension? This is critical for the efficient but robust design of multi-caisson systems where the jacket footprint is governed by the design of the most lightly loaded caisson. Although previous research has explored the effect of tensile loading, uncertainties remain in terms of the effects of average stress, cyclic amplitude and drainage regime. These areas require further scrutiny.

To ensure the experimental work is relevant there must be a careful consideration of scaling. Centrifuge testing, with a pore fluid of enhanced viscosity, has been adopted to ensure the self-weight stresses and the drainage regime reflect prototype behaviour (as demonstrated to be achieved by selecting a pore fluid with appropriate viscosity in Delwoolkar et al., 1999). The centrifuge experiments simulated in-situ conditions as closely as possible, by completing the full sequence of self-weight penetration, suction assisted installation, cyclic loading and extraction, all at in-situ stress levels.

The findings from these experiments are presented as two companion papers. This first paper describes the experimental arrangement and procedures, with the focus on suction installation and its effect on foundation stiffness, consideration of scaling and drainage, and the limiting capacity in tension. The second paper (Bienen et al., 2017) explores the vertical cyclic loading response, firstly by comparison with similar tests from the literature, to provide a perspective on the database of model suction caisson tests in sand to date. Thereafter, the focus is on the effects of drainage regime, average stress and cyclic amplitude, importantly including excursions into tension, partial contact of the lid with the soil plug and the implications on design of OWT foundations.

EXPERIMENTAL ARRANGEMENT AND PROCEDURES

All experiments were performed in the beam centrifuge at The University of Western Australia (Randolph et al., 1991) at an acceleration of 100g (defined at the sand surface).

Model and instrumentation

The tests were designed to simulate a jacket structure with three suction buckets supporting an OWT, through application of relevant load paths to a single foundation. The model caisson has a diameter $D = 80$ mm, skirt length $L = 40$ mm (i.e. an aspect ratio $L/D = 0.5$) and skirt thickness $t = 0.5$ mm (Figure 3). This is equivalent to a prototype caisson of $D = 8$ m and $L = 4$ m. Consideration was made of the flexural stiffness of the model caisson in the centrifuge compared with that of the equivalent prototype structure. The appropriate dimensionless group is Et/GD (Cox et al. 2014), where E is the Young's modulus of the caisson skirt, G is the representative shear modulus of the soil. Scaling of effective stress in the centrifuge results in values of G that are comparable at centrifuge and prototype scales.

The 0.5 mm skirt thickness corresponds to $t = 50$ mm at prototype scale, which although higher than used in practice, provides a broadly consistent flexural stiffness as the model caisson was fabricated from aluminium ($E = 70$ GPa) rather than steel ($E = 210$ GPa). The relative roughness of the caisson skirts R_a/d_{50} was 0.006 in the model, but may be around 0.03 in the field assuming slightly rusty steel.

The caisson features three pressure sensors: one pair of total and pore pressure transducers (PPT) are located on the caisson lid invert, and one additional total pressure transducer (TPT) measures fluid pressure at the top of the caisson lid. The caisson was connected to the vertical axis of an actuator via a rigid 13 mm diameter aluminium rod. An appropriate caisson weight – and cyclic load – was simulated using feedback control with input from a load cell that was positioned in series between the caisson and the rod. Where large cyclic loads were required, an 8 kN load cell was used, otherwise a 2 kN capacity load cell was employed. The displacement of the caisson was measured using a Linear Displacement Transducer (LDT) that was positioned between an independent fixed reference beam and the top of caisson lid. Figure 3 shows the model caisson and the experimental arrangement.

An electronic valve (shown in Figure 3) was used to vent the caisson during self-weight installation. The valve was closed remotely for the remainder of the test. A syringe pump (House, 2002) was used to perform the suction installation at enhanced gravity. The internal pump diameter is 50 mm, such that the pump plan area is 39% of the caisson plan area.

Sample preparation and pore fluid

Scaling the model caisson by a factor N (the centrifuge acceleration level), results in diffusion processes that occur N^2 times faster in the centrifuge compared to the equivalent prototype. It follows that for a water saturated centrifuge sample, loading frequencies would need to be very high to simulate prototype conditions. The alternative approach – routinely adopted for high frequency loading events such as earthquakes (Sharp et al., 2003; Abdoun et al., 2013; Lee et al., 2014) – is the use of a higher viscosity pore fluid with more moderate and technically achievable loading frequencies. This is the approach taken for the experimental work described here.

The tests were performed using Baskarp sand, with a particle size distribution typical for North Sea sands (Blaker and Andersen, 2015), and also matching the Baskarp sand underpinning the extensive cyclic loading database on dense sand at the Norwegian Geotechnical Institute (NGI) (Andersen and Berre, 1999). Figure 4 shows the particle size distribution of the Baskarp sand together with the Redhill 110 and Oakamoor HPF5 sands that were used in the cyclic tests reported by Kelly et al. (2006b), which are considered in the companion paper.

The sand samples were prepared by dry pluviation to create dense samples with a final depth of 205 mm. A total of six samples were prepared, of which the first five were saturated from the sample base with 100 cSt silicon oil. Sample 1 was used for trial tests not reported here. By selecting a pore fluid viscosity to match the enhanced gravity level in the centrifuge (N_g), the permeability with this pore fluid should be the same as that in the prototype (1g) with water. This is because the effects on Darcy's coefficient of permeability k are counteracted (Tan and Scott, 1985; Taylor, 1987; Delwoolkar et al., 1999). $k = gK/v$, where g is the gravitational acceleration, K the intrinsic permeability of the soil and v is the kinematic viscosity of the pore fluid, which for water is $10^{-6} \text{ m}^2/\text{s}$ or 1 cSt. Hence, the pore fluid in the first five samples is 100 times more viscous than water but the caisson penetration velocity in the model translates 1:1 to that of the prototype. The sixth sample was saturated with water containing approximately 3.5% cellulose ether (DOV, 2002) to obtain a significantly higher fluid viscosity of 660 cSt (the important point being the significant difference in viscosity, not the absolute value) at the testing temperature of 20° (as measured in a small sample using a viscometer, which confirmed the data from the manufacturer). This therefore allowed the influence of different resulting drainage regimes to be investigated. Due to the high viscosity of the water-cellulose ether solution, the saturation process from the base of the sixth sample could not be completed in a timely fashion. Instead, the box was flooded with the fluid and spun in the centrifuge at 100g for two days, to allow any trapped air to escape. The sample was believed to be fully saturated, with suction installation and cavitation limit for resistance under rapid extraction (as discussed later) performing as such. The use of two different pore fluid viscosities allowed investigation of the effects of permeability on the caisson behaviour. The relative density of the samples was $98 \pm 1\%$, as determined from global measurements of

the sample volume and mass (with values for each box provided in Table 1). A constant head of free fluid, of about 0.07 m, was maintained above the soil sample during the testing.

The maximum and minimum void ratios are $e_{\max} = 0.86$ and $e_{\min} = 0.57$ (obtained following the methodology outlined in Blaker et al., 2015) and the permeability for a water saturated sand sample with a relative density of 95% (i.e. close to that of the centrifuge samples) was found to be $k = 8.04 \times 10^{-5}$ m/s. The permeability was measured in a falling head test performed in a triaxial apparatus (but with no shearing of the sand specimen) with an anisotropic consolidation stress of 250 kPa and $K_0=0.45$ (similar to Andersen and Berre, 1999). The permeability was confirmed to be reduced by a factor of 100 when using the 100 cSt silicon oil in independent tests performed to support the centrifuge testing program. The peak mobilised angle of friction was found to be 44.5° (Andersen and Berre, 1999). The sample was sheared in compression by an increase in the axial force. Byrne and Houlsby (2004) report the peak friction angle of Baskarp sand to be reduced by 3° (as dilation is reduced) when saturated with 100 cSt silicon oil, based on data from NGI (1994). The friction angle is unaffected when the sand is saturated with water containing cellulose ether (Delwoolkar et al., 1999).

Four cone penetrometer tests (CPT) were performed in every sample using a centrifuge scale penetrometer with a diameter of 10 mm at a constant velocity of 1 mm/s. The tests were performed to identify potential variations between and/or within samples, and to provide the input data required for the caisson installation predictions (considered later in the paper). All CPT profiles of cone tip resistance, q_c , with penetration depth z normalised by the caisson skirt length L are shown in Figure 5.

The cone tip resistance was higher in the sample saturated with 660 cSt pore fluid, which may be due to differences in the drainage response generated as the cone was penetrated at the constant velocity of 1 mm/s.

Experimental program and procedure

The load paths were selected to be representative of the windward or leeward caisson (for a multi-footing OWT jacket structure) under operational conditions, which is reflected in the

wind and wave loading assumed. Neither the dimensions nor the loading conditions reflect any particular site. Rather, they are considered representative for a generic jacket supported 8 MW turbine, in 40 m water depth, in the North Sea with a dense sand seabed. In the evaluation of the load paths, which was performed with an integrated in-house code featuring aero- and hydrodynamic, structural and macro-element foundation models (Bienen and Cassidy, 2006; Senders, 2008), the OWT was positioned such that one caisson faced windward, the other two leeward, as this will result in the maximum change in (vertical) loading on the lightly loaded foundation, with the caisson spacing chosen such that cyclic excursions into tension of the windward caisson are expected.

The experiments were performed according to the following procedure, which is illustrated schematically in Figure 6:

- 1) Self-weight installation under load control, achieved using feedback from the load cell to change the displacement accordingly, with a slow set-down as is adopted in practice so as not to disturb the sand bed. The self-weight was assumed to comprise of 120 t per caisson and 700 t for the jacket. This amounts to a vertical load V of 3.5 MN per caisson in prototype scale, 350 N in model scale and is equivalent to an applied stress $V/A = 70$ kPa, where A is the plan area of the suction caisson. In the test, the caisson penetration was achieved under load control at a rate of 1 N/s without stopping the centrifuge. When the load reached the targeted 350 N the vent valve was closed remotely.
- 2) Suction-assisted installation followed, with pumping at a constant syringe pump flow rate while the load was held constant to simulate the caisson self-weight.
- 3) Additional self-weight was then applied to the caisson, to model the installation of the wind turbine on the jacket. The vertical load was hence increased to 585 N (i.e. an applied stress of 116 kPa) to represent the full self-weight of the OWT per caisson including tower, nacelle and rotor.
- 4) Pre-shearing was then performed, a procedure by which small amplitude cyclic loading is applied. The rationale for including a pre-shearing stage was an intent to model cyclic events accompanied by drainage prior to the investigated cyclic event and to emulate a bedding-in process in the field (Andersen, 2015). Therefore 400

small amplitude loading cycles (of ± 6 kPa) were applied around an average stress of 116 kPa. Pre-shearing events have also been applied in laboratory element tests, such as those forming the cyclic behaviour database for Baskarp sand (Andersen and Berre, 1999).

- 5) Cyclic loading, performed under load control. The average vertical load was adjusted to reflect that of a windward/leeward caisson in operation, i.e. with consideration of self-weight and wind on the OWT. This resulted in a vertical average load of 40 N in the model (8 kPa) on the windward caisson and 2500 N (500 kPa) on a leeward caisson. Cyclic loading is the focus of the companion paper (Bienen et al. 2017).
- 6) At the end caisson extraction was performed under displacement control, prior to which any excess pore pressure was allowed to dissipate. Caisson extraction was performed at a rate of 0.001 mm/s or 3 mm/s to explore pull-out capacity approaching drained and undrained behaviour, respectively.

All operations were completed without stopping the centrifuge.

The changes in vertical load prior to the stages of pre-shearing and cyclic loading were applied as step changes, following which any excess pore pressure was allowed to dissipate. This provided an opportunity to assess the in situ drainage characteristics. The objective in the cyclic loading phase of the tests was to replicate realistic drainage conditions. This was achieved using a pore fluid with a viscosity that was either 100 or 660 times that of water and a cyclic loading frequency of 0.5 Hz at model scale (except the repeat loading sequences in tests 4-3 and 6-6, which were performed at 0.25 Hz).

Table 1 summarises the test details. Where the cyclic loading history was repeated, this was done immediately following the conclusion of the previous load application, without any wait period or adjustment of position of the caisson. The naming convention lists the sample number, followed by the test number in that sample, e.g. 6-5 refers to the fifth test performed in sample six. Each test was performed at a new site. The minimum clear spacing between tests was one caisson diameter, such that such that the tests were not expected to influence each other. The loading history (LC1~11) applied in each test is shown schematically in Table 1. 20 tests in total were performed with:

- Tests 2-1, 2-2 and 2-3 investigating the effect of suction installation rate on the compressive cyclic loading response of the caisson,
- 3-2, 6-4, 6-5 and 6-6 exploring the drained frictional tensile capacity,
- 4-3 and 6-6 providing context to the database already in the public domain, and
- the remaining tests investigating the effects of drainage regime, cyclic average stress and amplitude on the caisson response as the load cycles into tension.

Cyclic vertical loading of an offshore foundation will be irregular in nature and amplitude, with the loading frequencies continuously changing depending on the metocean conditions. In this study and as in design, the loading characteristics are simplified to sinusoidal cyclic loading with constant frequency.

All tests are discussed in this paper in terms of installation, drainage characteristics and extraction. The response of the caisson during cyclic loading is discussed in the companion paper.

RESULTS AND DISCUSSION

The experimental results are presented in non-dimensional form unless stated otherwise.

Suction installation and its influence on caisson response under subsequent cyclic loading

All installation data are summarised in Table 2 and Figure 7, providing the normalised penetration depths under self-weight penetration, after suction installation, before and after pre-shearing, and prior to the application of cyclic loading (with any changes related to the magnitude of applied stress as indicated in Table 2). The penetration depth is normalised by the skirt length, which is felt to be an appropriate representative length, rather than the diameter (as $L/D = 0.5$ it is simple to convert to z/D).

Figure 8 shows results from installations with the pumping flow rate differing by three orders of magnitude to explore the effect of different constant pumping rates on the installation response. Despite the significant difference in pumping rate, very similar responses in terms of normalised suction $p/\gamma'D$ at the caisson lid invert were measured, where p is the differential

pressure across the lid, γ' the effective unit weight of the soil and D the caisson diameter. Note that for presentation, the graphs show the change in skirt penetration during the suction installation phase only. If the process was undrained the three pumping flow rates of 39.3 mm³/s, 392.7 mm³/s and 3,927.0 mm³/s (in model scale) would correspond to installation rates of 0.0078 mm/s, 0.078 mm/s and 0.78 mm/s. It is therefore expected that the caisson velocity will start at this rate and then reduce as seepage occurs given the total extracted flow is fixed. As the caisson penetration velocity is the same in the model with enhanced pore fluid viscosity (100 cSt) as in the prototype with water as pore fluid, this implies a prototype installation of 2.5 m of skirt length, in 8.9 hours for the intermediate pumping flow rate, which is a realistic timescale for installation. The lower and higher pumping rates explore the potential for adverse or beneficial behaviour as examined later in the paper.

There are three methods reported in the literature that can be used for calculations of suction pressure with penetration (Houlsby and Byrne, 2005; Andersen et al., 2008; Senders and Randolph, 2009). The Houlsby and Byrne method follows a classical approach and relates the tip and frictional resistance to effective stresses. The prediction depends on the friction angle ϕ , the ratio of effective vertical to horizontal stresses at the skirt K , the interface friction angle δ , the ratio of permeability within the soil plug to outside the caisson $k_{\text{inside}}/k_{\text{outside}}$, and a down-drag stress enhancement factor m . Andersen et al. (2008) propose both a bearing capacity as well as a CPT correlation approach, and the latter is used here. This relates the skirt tip resistance and wall friction to the cone tip resistance via empirical correlation factors k_{tip} and k_{side} . The permeability ratio $k_{\text{inside}}/k_{\text{outside}}$ can also be selected. The Senders and Randolph CPT correlation method, in contrast, assumes a permeability ratio $k_{\text{inside}}/k_{\text{outside}}$ of 1. The empirical factors for tip resistance and wall friction are termed here k_p and k_f , respectively.

Predictions by the three methods, with the input parameters listed in Table 3, are included in Figure 8. The three methods provide similar predictions and reassuringly good agreement with the measured data. Calculations using these methods have also been shown to agree well with records of field installations such as at Draupner E and Sleipner platforms as well as data from laboratory tests (Houlsby and Byrne, 2005; Andersen et al., 2008; Senders and Randolph, 2009). The self-weight penetration is predicted at $z/L = 0.53$ (Andersen et al.,

2008 using an average CPT profile; 0.31 and 0.74 using the min/max CPT profiles, with these three predictions included in Figure 7), 0.48 (Senders and Randolph, 2009) and 0.52 (Houlsby and Byrne, 2005, using $\phi = 41.5^\circ$ to account for the reduced friction angle in silicon oil saturated sand).

The differing trend of the prediction of the required suction using Andersen et al. is attributed to the empirical contours of normalised penetration resistance, particularly at larger skirt penetration depths. The parameters k_{tip} and k_{side} play a significantly lesser role in defining the curvature of the prediction.

It is widely acknowledged that suction installation alters the effective stresses in sand and likely also the relative density and permeability of the soil plug. Increased permeability in the soil plug ($k_{inside}/k_{outside} > 1$) can be taken into account in the methods by Houlsby and Byrne and Andersen et al. However, the best predictions were achieved with $k_{inside}/k_{outside} = 1$. This suggests that the soil plug as a whole was not significantly loosened by the suction installation process, which is also supported by the observed final penetration depths. This contrasts with observations from the 1g tests reported in Jostad et al. (1997) and Andersen et al. (2008).

Despite registering similar suction at the PPT location beneath the lid, the installation responses differed significantly, with the lowest pumping rate resulting in premature refusal and hence incomplete skirt penetration (even though suction in this test commenced from a comparatively high self-weight penetration and the pumping rate was increased successively when the caisson penetration rate slowed markedly). Figures 9 and 10 show the caisson penetration rate during the suction installation phase, for different pumping rates in the same sample (Fig. 9) and for the same pumping rate in sand saturated with different viscosity pore fluid (Fig. 10).

The lowest pumping rate was sufficient to mobilise the required suction (i.e. the predicted suction as shown in Figure 8) but failed to decrease the effective stresses around the skirt tip sufficiently for complete skirt penetration. At the end of the test the pumping rate was effective only in extracting the seepage flow. This is in line with what would be predicted

using the Houlsby and Byrne (2005) calculation method, and also with experimental observations (Tran, 2005). The intermediate and fast pumping rates resulted in successful suction installation ($z/L \approx 1$), with the velocity of caisson penetration differing slightly with depth due to the differing seepage volumes that must be extracted. The same is true for suction installations at the intermediate pumping rate in samples saturated with different viscosity pore fluid. In the sample saturated with 100 cSt pore fluid, the caisson penetration rate decreases markedly with depth (Fig. 10). In contrast, the caisson penetration rate remains approximately constant over the entire suction installation phase for the 660 cSt pore fluid – effectively there is no seepage flow and the pumping rate corresponds to the caisson skirt volume penetrating into the soil. Figure 10 also shows the penetrated caisson volume normalised by the pump flow rate. A value of 1 implies complete transferral of pumping to advancing the caisson (i.e. no seepage flow). This link between the pumping rate, drainage characteristics and suction is described in Houlsby and Byrne (2005) through a series of simplified calculations. The results of these calculations are plotted on both Figure 9 and 10 showing good agreement. Note that the calculations must account for the effect of increased viscosity on permeability and hence seepage flow under the higher accelerations in the centrifuge (as discussed previously). The results described here are also consistent with the work by Cotter (2009) on caissons in homogeneous sands at model scale in the laboratory.

Figure 7 shows that the final penetration following suction installation in the majority of the tests is around $z/L = 0.9$, suggesting slight soil plug heave during this process. Some tests penetrate to $z/L = 1$. However prior to the pre-shearing phase, following the loading to 116 kPa, most of the caissons penetrate closer to $z/L = 1$. No or very limited accumulated displacement was measured during the pre-shearing phase.

In order to evaluate the effect of the different suction installation history on the subsequent caisson response, Figure 11 shows the normalised unloading stiffness under onerous compressive cyclic loading following pre-shearing for the three tests in which the pumping rate differed by two orders of magnitude (Tests 2-1, 2-2, 2-3). While the unloading stiffness increases by a factor of approximately three initially (which will influence the system stiffness, albeit by a lower factor), the effect of pumping rate on the development of stiffness with cycle number is not discernible.

However, Figure 12 shows that the pumping rate may have a slight effect on the accumulation of displacements during subsequent cyclic loading. The suction installation at the fastest rate resulted in the same skirt penetration as the intermediate rate but slightly lower normalised displacements. In contrast, the largest normalised displacements were measured following the slowest suction installation (Test 2-2, 392.7 mm³/s). In this test the caisson skirt penetration prior to cyclic loading was the highest of all three tests. These observations are based on a limited set of tests and this aspect warrants further investigation. The intermediate model pumping flow rate of 392.7 mm³/s was selected for the remainder of the testing programme. This pumping flow rate results in caisson installation times that relate closely to the prototype, as discussed above.

In summary, the tests described above indicate that the change, due to penetration, in soil state and permeability of the soil plug overall appears to be small. The most significant effect of the pumping rate is the achieved penetration depth, with a minimum pumping flow rate required for successful suction installation. This can be assessed using the calculations by Houlsby and Byrne (2005).

Drainage conditions

The loading sequence in the centrifuge tests allowed characterisation of the consolidation behaviour, with step changes in the vertical load prior to pre-shearing and cyclic loading, followed by dissipation of excess pore pressures. Figure 13 shows the pore pressure dissipation time histories following a step change in the load, showing the difference in response for the two pore fluids. Pore pressure dissipation is evidently faster for the sample saturated with silicon oil, reflecting a higher permeability. This is more clearly shown by the inset in Figure 13, which summarises the time required to achieve 50% dissipation.

Therefore, during the cyclic loading stage that was performed at a model cyclic loading frequency of 0.5 Hz, i.e. a cyclic period of 2 s and hence load application over 0.5 s, the response with 660 cSt pore fluid (cellulose ether) is expected to be (near) undrained. However, with the lower pore fluid viscosity (100 cSt in silicon oil), a partially drained response is expected.

Limiting capacities

The compressive capacity for the caisson is large in the dense sand (for this case the estimate is in excess of 6 MPa) and is not expected to be fully mobilised. The investigation of the tensile loading and associated displacements, which forms the focus of the companion paper (Bienen et al., 2017), requires knowledge of the drained and undrained limiting capacities in tension. These were probed at the completion of each test (i.e. most results include a cyclic loading history; see Table 1) under displacement control with the valve closed at a constant rate of 0.001 or 3 mm/s (i.e. differing by three orders of magnitude), which were expected to generate drained and (and close to) undrained behaviour respectively. As the velocity scales 1:1 between the centrifuge model and the prototype, these rates correspond to 0.0036 and 10.8 m/h, respectively.

Figure 14a shows that drained skirt friction is mobilised within $\sim 0.003D$ of upward displacement. In Tests 6-4, 6-5 and 6-6, the extraction rate was increased once the drained frictional limiting capacity was reached (to save time in the testing programme) and consequently only the drained portion of the extraction response is shown on Figure 14a. Without a cyclic loading history apart from pre-shearing (Test 3-2), the results agree well with the Housby et al. (2005b) prediction (also shown on Figure 14), which is based on similar principles as the Housby and Byrne (2005) installation calculation. The following observations are made in the other three tests:

- Test 6-6 recorded the highest self-weight penetration and hence the least suction penetration. The loading history featured cycling mostly in compression, around a large compressive average stress, and resulted in settlement. The measured frictional extraction resistance exceeds that predicted, indicating densification during the test.
- Tests 6-4 and 6-5 had similar cyclic loading amplitudes, but different average stresses. The average stress in 6-4 was 0 kPa, which resulted in upward movement of the caisson during cycling and the lowest frictional extraction resistance. The compressive average stress in test 6-5 changed the overall response to settlement, and the subsequent frictional extraction resistance exceeds the predicted.

Despite the clear trend in this set of results, further data is required to fully establish the effect of the loading history on the drained frictional capacity and exclude natural experimental variation.

The capacity mobilised at the fast uplift rate appears to be limited by cavitation in most cases (Houlsby et al. 2005b). In the tests with 660 cSt pore fluid (Tests 6-1, -2, -4, -5, -6), the response was undrained, and cavitation was always reached. For the extraction in the samples saturated with silicon oil there was some drainage (also identified by the lower t_{50} times) so that the uplift capacity was slightly lower than the cavitation limit, but still much greater than the drained frictional capacity. The mobilisation distance of $\sim 0.084D$ is approximately 30 times higher than the drained friction mobilisation distance.

Table 4 provides a summary of the parameters used in calculating the drained and undrained tensile capacities. The drained tensile capacity consists of internal and external skin friction (Houlsby et al., 2005b), following the same approach as the prediction of installation under self-weight, but now with a reduction in the vertical stress due to up-drag (rather than down-drag in the installation calculation). Cavitation with liquefaction limits the undrained tensile capacity. The values of $K_{tan}\delta$ and m were identical to those used in the installation predictions.

The preceding discussion has highlighted the importance of knowledge of the in situ permeability – which affects all stages of the design life of a suction caisson - and the companion paper demonstrates this further. Site investigation programs should include permeability measurements. These can be performed as part of penetrometer tests in situ in low permeability soils. For clean sand this is more difficult because of the fast drainage time and a tool that can generate excess pore pressure may be required. The information can be used to obtain an estimate of t_{50} , which allows for a site specific assessment of the drainage response.

CONCLUDING REMARKS

This paper has described a series of tests, performed on a geotechnical centrifuge, that explore the behaviour of suction caissons under conditions relevant for offshore wind

turbines. The tests focus on installation behaviour, cyclic loading response and the limiting capacities for caisson extraction.

The suction required for caisson installation in dense sand measured in the centrifuge tests is well matched by existing methods, with appropriate choice of input parameters. The test results show that a successful installation will require a minimum pumping rate to ensure that effective soil stresses around the skirt tip are sufficiently reduced. Therefore, to ensure appropriate specification of pumping systems it will be important to obtain in-situ estimates of the soil drainage characteristics. This may require new site investigation procedures and/or tools.

In the centrifuge tests, full skirt penetration was achieved without significant loosening of the soil plug. Although this observation was not confirmed by direct investigation of the plug, the conclusion is supported by (i) the use of a permeability ratio of 1 for prediction of the suction installation and (ii) little observed difference in the caisson response to an onerous cyclic loading history following different installation rates. The limiting capacity in tension could be predicted by existing calculation methods, though there were some effects caused by the cyclic loading history applied prior to extraction. The undrained capacity appeared to be bounded by the cavitation limit for the rates applied. Implications of cyclic loading into tension, and the role of the frictional limit, is explored in detail in the companion paper.

ACKNOWLEDGEMENTS

This work forms part of the activities of the Centre for Offshore Foundation Systems (COFS), which is currently supported as one of the primary nodes of the Australian Research Council (ARC) Centre of Excellence for Geotechnical Science and Engineering and as a Centre of Excellence by the Lloyd's Register Foundation. Lloyd's Register Foundation helps to protect life and property by supporting engineering-related education, public engagement and the application of research. This support is gratefully acknowledged.

Notation

A caisson area
d₅₀ particle size

D	caisson diameter
D_r	relative density
e_{\max}	maximum void ratios
e_{\min}	minimum void ratio
E	Young's modulus
g	gravitational acceleration
G	shear modulus
k	Darcy's coefficient of permeability
k_f	empirical correlation factor
k_{inside}	permeability inside caisson
k_{outside}	permeability outside caisson
k_p	empirical correlation factor
k_{side}	empirical correlation factor
k_{tip}	empirical correlation factor
K	intrinsic permeability of the soil
K_0	horizontal earth pressure coefficient at rest
L	caisson skirt length
m	multiple of diameter over which vertical stress is enhanced
N	centrifuge acceleration level
p	differential pressure across the lid
q_c	cone tip resistance
R_a	roughness
t	skirt thickness
t_{50}	time required for 50% of consolidation
V	vertical load
z	penetration depth
δ	interface friction angle
γ'	effective soil unit weight
ϕ	friction angle
v	kinematic viscosity

REFERENCES

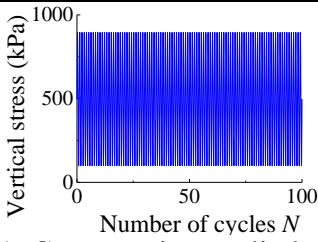
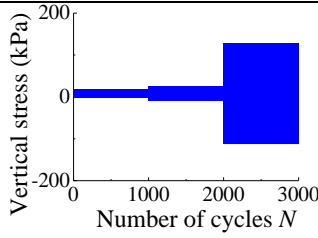
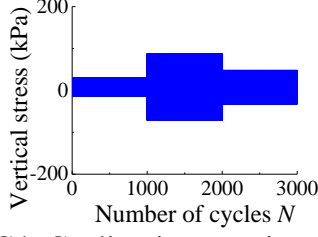
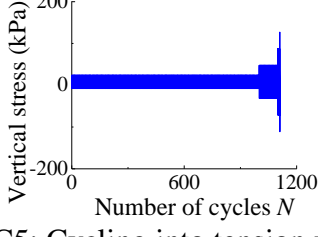
- Abdoun, T., Gonzalez, M.A., Thevanayagam, S., Dobry, R., Elgamal, A., Zeghal, M., Mercado, V.M., El Shamy, U. (2013). Centrifuge and large-scale modeling of seismic pore pressures in sands: Cyclic strain interpretation. *Journal of Geotechnical and Geoenvironmental Engineering*, Vol. 139, No 8, pp 1215-1234.
- Andersen, K.H. (2015). Cyclic soil parameters for offshore foundation design. The Third ISSMGE McClelland lecture. *Frontiers in Offshore Geotechnics III (ISFOG)*, pp. 5-82.
- Andersen, K.H., Berre, T. (1999). Behaviour of a dense sand under monotonic and cyclic loading. *Proc. ECMGE XII Geotechnical Engineering for Transportation Infrastructure*, Vol. 2, pp. 667-676.
- Andersen, K.H., Murff, J.D., Randolph, M.F., Clukey, E., Erbrich, C., Jostad, H.P., Hansen, B., Aubeny, C., Sharma, P., Supachawarote, C. (2005). Suction anchors for deepwater applications. *Proc. International Symposium on Frontiers in Offshore Geotechniques (ISFOG)*, pp. 3–30.
- Andersen, K.H., Jostad, H.P. and Dyvik, R. (2008). Penetration resistance of offshore skirted foundations and anchors in dense sand. *Journal of Geotechnical and Geoenvironmental Engineering (ASCE)*, Vol 134, No. 1, pp. 106-116.
- Bienen, B., Cassidy, M.J. (2006). Advances in the three-dimensional fluid-structure-soil interaction analysis of offshore jack-up structures. *Marine Structures*, Vol. 19, No. 2-3, pp. 110-140.
- Bienen, B., Klinkvort, R.T., O'Loughlin, C., Zhu, F., Byrne, B.W. (2017). Suction caissons in dense sand, Part II: Vertical cyclic loading into tension. *Géotechnique*, submitted.
- Blaker, Ø., Andersen, K.H. (2015). Shear strength of dense to very dense Dogger Bank sand. *Frontiers in Offshore Geotechnics III (ISFOG)*, pp. 1167-1172.
- Blaker, Ø., Lunne, T., Vestgården, T., Krogh, L., Thomsen, N.V., Powell, J.J.M., Wallace, C.F. (2015). Method dependency for determining maximum and minimum dry unit weights of sands. *Frontiers in Offshore Geotechnics III (ISFOG)*, pp. 1159-1166.
- Bye, A., Erbrich, C., Rognlien, B., Tjelta, T.I. (1995). Geotechnical design of bucket foundation. *Offshore technology conference, OTC 7793*, pp. 869-883.

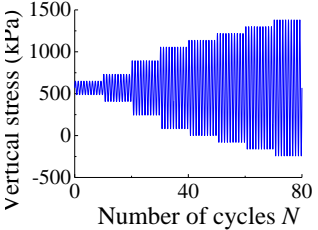
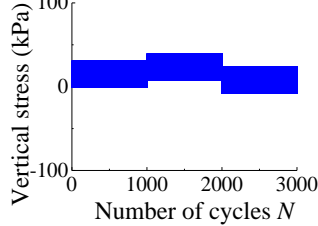
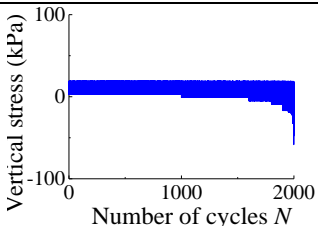
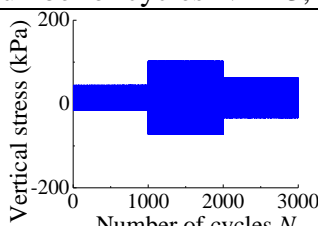
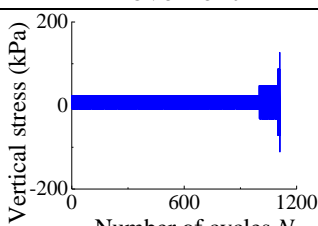
- Byrne, B.W. (2000). Investigations of suction caissons in dense sand. DPhil Thesis, Department of Engineering Science, The University of Oxford, UK.
- Byrne, B.W., Houlsby, G.T. (2002). Experimental investigations of the response of suction caissons to transient vertical loading. *Journal of Geotechnical Engineering (ASCE)*, Vol. 128, No 11, pp. 926-939.
- Byrne, B.W., Houlsby, G.T. (2004). Experimental investigations of the response of suction caissons to transient combined loading. *Journal of Geotechnical and Geoenvironmental Engineering (ASCE)*, Vol. 130, No 3, pp 240-253.
- Cotter, O.J. (2009). The installation of suction caisson foundations for offshore renewable energy structures. DPhil Thesis. The University of Oxford.
- Cox, J.A., O'Loughlin, C., Cassidy, M.J., Bhattacharya, S., Gaudin, C., Bienen, B. (2014). Centrifuge study on the cyclic performance of caissons in sand. *International Journal of Physical Modelling in Geotechnics*, Vol. 14, No. 4, pp. 99-115.
- Dewoolkar, M.M., Ko, H.-Y., Stadler, A.T., Astaneh, S.M.F. (1999). A substitute pore fluid for seismic centrifuge modelling. *Geotechnical Testing Journal*, Vol. 22, No. 3, pp. 196-210.
- DOV (2002). *Methocel Cellulose ethers*. Technical Handbook.
- Eide, O., Andersen, K.H. (1984). *Foundation engineering for gravity structures in the Northern North Sea*. Publication No. 154, Oslo, Norwegian Geotechnical Institute.
- Hansen, B., Nowacki, F., Skomedal, E., Hermstad, J. (1992). Foundation design: Troll platform. Proc. Int. Conf. on Behaviour of Offshore Structures, BOSS '92, Bentham, London, 921-936.
- Houlsby, G.T., Byrne, B.W. (2005). Calculation procedures for installation of suction caissons in sand. *Geotechnical Engineering (ICE)*, Vol. 158, No 3, pp 135-144.
- Houlsby, G.T., Ibsen, L.B., Byrne, B.W (2005a). Suction Caissons for Wind Turbines. *Proc. International Symposium on Frontiers in Offshore Geotechnics (ISFOG)*, pp 75-94.
- Houlsby, G.T., Kelly, R.B., Byrne, B.W. (2005b). The Tensile Capacity of Suction Caissons in Sand under Rapid Loading. *Proc. International Symposium on Frontiers in Offshore Geotechnics (ISFOG)*, pp 405-410.

- Houlsby, G.T., Kelly, R.B., Huxtable, J., Byrne, B.W. (2006). Field trials of suction caissons in sand for offshore wind turbine foundations. *Géotechnique*, Vol. 56, No. 1, pp 3-10.
- House, A.R. (2002). Suction caisson foundations for buoyant offshore foundations. PhD Thesis, The University of Western Australia.
- Ibsen, L.B. (2008). Implementation of a new Foundations Concept for Offshore Wind Farms. *Proc. Nordisk Geoteknikermøte nr. 15: NGM 2008*, Nordisk geoteknikermøte, Sandefjord. Norsk Geoteknisk Forening, pp. 19-33.
- Jostad, H.P., Andersen, K.H., Tjelta, T.I. (1997) Analyses of skirted foundation and anchors in sand subjected to cyclic loading. *Proc. International conference on the behaviour of offshore structures*, Vol. 1, pp.149-162.
- Kallehave, D., Thilsted, C.L., Troya, A. (2015) Observed variations of monopole foundation stiffness. *Frontiers in Offshore Geotechnics (ISFOG) III*, pp. 717-722.
- Kelly, R.B., Houlsby, G.T. and Byrne, B.W. (2006a). A comparison of field and laboratory caisson tests in sand and clay. *Géotechnique* 56, No 9, pp 617-626.
- Kelly, R.B., Houlsby, G.T., Byrne, B.W. (2006b). Transient vertical loading of model suction caissons in a pressure chamber. *Géotechnique*, Vol. 56, No 10, pp 665–675.
- LeBlanc, C. (2009). *Design of Offshore Wind Turbine Support Structures: Selected topics in the field of geotechnical engineering*. PhD Thesis, Aalborg University, Denmark.
- Lee, C. J., Chen, H. T., Lien, H. C., Wei, Y. C., Hung, W. Y. (2014). Centrifuge modeling of the seismic responses of sand deposits with an intra-silt layer. *Soil Dynamics and Earthquake Engineering*, Vol. 65, pp 72-88.
- NGI (1994). *Sleipner T—Special laboratory testing. Report No. 932514-1*, Norwegian Geotechnical Institute, Oslo, Norway.
- Peire, K., Nonneman H., Bosschem, E. (2009). Gravity based foundations for the Thornton Bank Offshore Wind Farm, *Terra et Aqua*, No 115, pp 19–29.
- Randolph, M.F., Jewell, R.J., Stone, K.J.L., Brown, T.A. (1991). Establishing a new centrifuge facility. *Proc. Centrifuge 1991*, pp. 2-9.
- Senders, M. (2008). *Suction caissons in sand as tripod foundations for offshore wind turbines*. PhD Thesis, The University of Western Australia.

- Senders, M., Randolph, M.F. (2009). CPT-based method for the installation of suction caissons in sand. *Journal of Geotechnical and Geoenvironmental Engineering (ASCE)*, Vol. 135, No 1, pp 14-25.
- Sharp, M.K., Dobry, R., Abdoun, T. (2003). Liquefaction centrifuge modeling of sands of different permeability. *Journal of Geotechnical and Geoenvironmental Engineering*, Vol. 129, No. 12, pp 1083-1091.
- Tan, T.-S. and Scott, R.F. (1985). Centrifuge scaling considerations for fluid-particle systems. *Geotechnique* Vol 35, No 4, pp 461-470.
- Taylor, R.N. (1987) Discussion of “Tan, T.-S. and Scott, R.F. (1985). Centrifuge scaling considerations for fluid-particle systems.” *Geotechnique* Vol 37, No 1, pp 131-133.
- Tjelta, T.I. (2015). The suction foundation technology. *Frontiers in Offshore Geotechnics (ISFOG) III*, pp. 85-93.
- Tjelta, T.I. Guttormsen, T.R., Hermstad, J. (1986). Large-scale penetration test at a deepwater site. *Offshore Technology Conference (OTC)*, OTC5103.
- Tran, M.N. (2005). *Installation of suction caissons in dense sand and the influence of silt and cemented layers*. PhD Thesis, The University of Sydney, Australia.
- Zhu, B., Byrne, B.W., Houlsby, G.T. (2013). Long-term lateral cyclic response of suction caisson foundations in sand. *Journal of Geotechnical and Geoenvironmental Engineering (ASCE)*, Vol. 139, No. 1, pp. 73-83.

Table 1: Details of the centrifuge experiments

Test name	Pore fluid	D_r (%)	Model pumping flow rate (mm^3/s)	Loading history	Extraction rate (mm/s)
2-1	100 cSt silicon oil	98	392.7	 <p>LC1: Compressive cyclic loading</p>	3
2-2			39.3 increasing to 294.5		3
2-3			3,927.0		3
3-1		97	392.7	LC2: Cycling into tension with compressive average stress	3
3-2				Drained frictional capacity without cyclic loading history	0.001
3-3				 <p>LC3: Cycling into tension with compressive average stress</p>	3
4-1				 <p>LC4: Cycling into tension with compressive average stress</p>	3
4-2				99	 <p>LC5: Cycling into tension with compressive average stress. 33 sequences of LC5 applied, total number of cycles $N = 36,724$</p>

4-3			 <p>LC11: Cyclic loading with large compressive average stress, 2 sequences of LC11 applied (at 0.5 Hz, 0.25 Hz).</p>	3
5-1			 <p>Initial loading of -6 ± 16 kPa abandoned after $N = 82$, then LC6: compressive average stress due to significant upward movement</p>	3
5-2		98	 <p>LC10: Cyclic loading with constant maximum stress, 11 sequences of LC10 applied, total number of cycles $N = 23,283$</p>	3
5-3			 <p>Initial loading of 0 ± 6 kPa abandoned after $N = 28$, then LC7: compressive average stress due to significant upward movement</p>	3
6-1	660 cSt water with cellulose ether	98	 <p>LC5: Cycling into tension with</p>	3

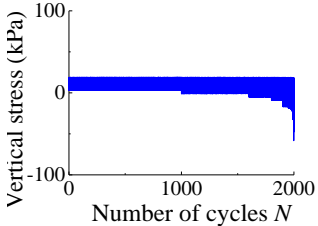
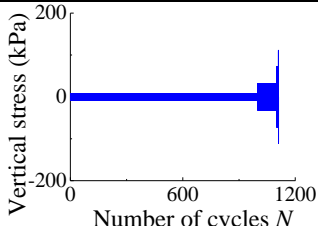
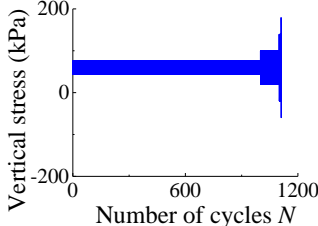
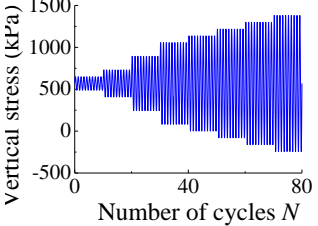
				compressive average stress, 5 sequences of LC5 applied, total number of cycles $N = 5,587$	
6-2				 <p>Vertical stress (kPa)</p> <p>Number of cycles N</p> <p>LC10: Cyclic loading with constant maximum stress, 14 sequences of LC10 applied, total number of cycles $N = 28,335$</p>	3
6-4				 <p>Vertical stress (kPa)</p> <p>Number of cycles N</p> <p>LC8: Cyclic loading into tension with 0 kPa average stress</p>	0.001, increased to 3 once drained frictional capacity was reached
6-5				 <p>Vertical stress (kPa)</p> <p>Number of cycles N</p> <p>LC9: Cycling into tension with larger compressive average stress, 6 sequences of LC9 applied, total number of cycles N $= 30,098$</p>	0.001, increased to 3 once drained frictional capacity was reached
6-6				 <p>Vertical stress (kPa)</p> <p>Number of cycles N</p> <p>LC11: Cyclic loading with large compressive average stress, 2 sequences of LC11 applied (at 0.5 Hz, 0.25 Hz).</p>	0.001, increased to 3 once drained frictional capacity was reached

Table 2: Penetration depths

Test name	Pore fluid	Model pumping flow rate (mm ³ /s)	Penetration depth z/L					
			Under self-weight	After suction installation	Pre-shear		Before cycling (change in applied stress)	
					Before	After		
2-1	100 cSt silicon oil	392.7	0.35	0.76	0.78	0.78	1.11 (116 → 500 kPa)	
2-2		39.3~294.5	0.57	0.83	0.95	0.96	1.32 (116 → 500 kPa)	
2-3		3,927.0	0.36	0.93	0.96	0.96	1.10 (116 → 500 kPa)	
3-1		392.7		0.64	1.07	1.10	1.10	1.10 (116 → 8 kPa)
3-2				0.57	0.89	0.98	0.99	-
3-3				0.54	0.79	0.90	0.90	0.90 (116 → 8 kPa)
4-1				0.50	0.97	0.99	0.99	0.99 (116 → 8 kPa)
4-2				0.58	1.02	1.04	1.04	1.04 (116 → 8 kPa)
4-3				0.45	0.93	0.94	0.94	1.14 (116 → 569 kPa)
5-1				0.45	0.92	0.94	0.95	0.95 (116 → -6 kPa)
5-2				0.54	0.98	0.99	1.00	1.00 (116 → 20 kPa)
5-3				0.49	0.87	0.87	0.89	0.87 (116 → 0 kPa)
6-1				660 cSt water with cellulose ether		0.32	0.99	1.00
6-2		0.32	1.00			1.01	1.01	1.01 (116 → 20 kPa)
6-4		0.35	1.00			1.01	1.01	1.01 (116 → 0 kPa)
6-5	0.27	0.86	0.87			0.87	0.87 (116 → 60 kPa)	
6-6	0.40	0.93	0.93			0.93	1.18 (116 → 569 kPa)	

The penetration achieved under self-weight falls within the range $z/L = 0.27$ to 0.64 and is correlated with the CPT resistance.

Table 3: Input parameters for penetration predictions

Reference	Approach	Parameter	Value
Houlsby & Byrne (2005)	Effective stress approach	$K \tan \delta$	0.5
		ϕ	41.5°
		m	1.3
		$k_{\text{inside}}/k_{\text{outside}}$	1.0
Andersen et al. (2008)	CPT correlation	k_{side}	0.0053
		k_{tip}	1.2
		$k_{\text{inside}}/k_{\text{outside}}$	1.0
Senders & Randolph (2009)	CPT correlation	k_f	0.003
		k_p	0.3

Table 4: Input parameters for extraction predictions (Houlsby et al. 2005b)

	Parameter	Value
Drained	$K \tan \delta$	0.5
	n	0.98
	m	1.3
Undrained	$K \tan \delta$	0.5
	m	1.3

Figure 1: Offshore wind turbine with jacket substructure supported by suction caissons with indicative dimensions.

Figure 2: Suction caisson installation in sand.

Figure 3: Model caisson and experimental arrangement in the centrifuge.

Figure 4: Particle size distributions.

Figure 5: CPT profiles.

Figure 6: Testing procedure.

Figure 7: Installation history in terms of normalised penetration depth of all tests, with predictions based on Andersen et al. (2008).

Figure 8: Predicted required suction compared with actual installation response, a) low, b) medium, c) fast pumping flow rate.

Figure 9: Installation response for pumping flow rates spanning three orders of magnitude in silicon oil saturated samples, a) overview, b) enlarged view.

Figure 10: Installation response for the same model pumping flow rate of $392.7 \text{ mm}^3/\text{s}$ in samples with different viscosity pore fluid.

Figure 11: Normalised unloading stiffness under cyclic compressive loading.

Figure 12: Effect of suction installation rate on displacement accumulation.

Figure 13: Consolidation characteristics in centrifuge tests.

Figure 14: (a) Drained and (b) undrained extraction resistance, compared with predictions.

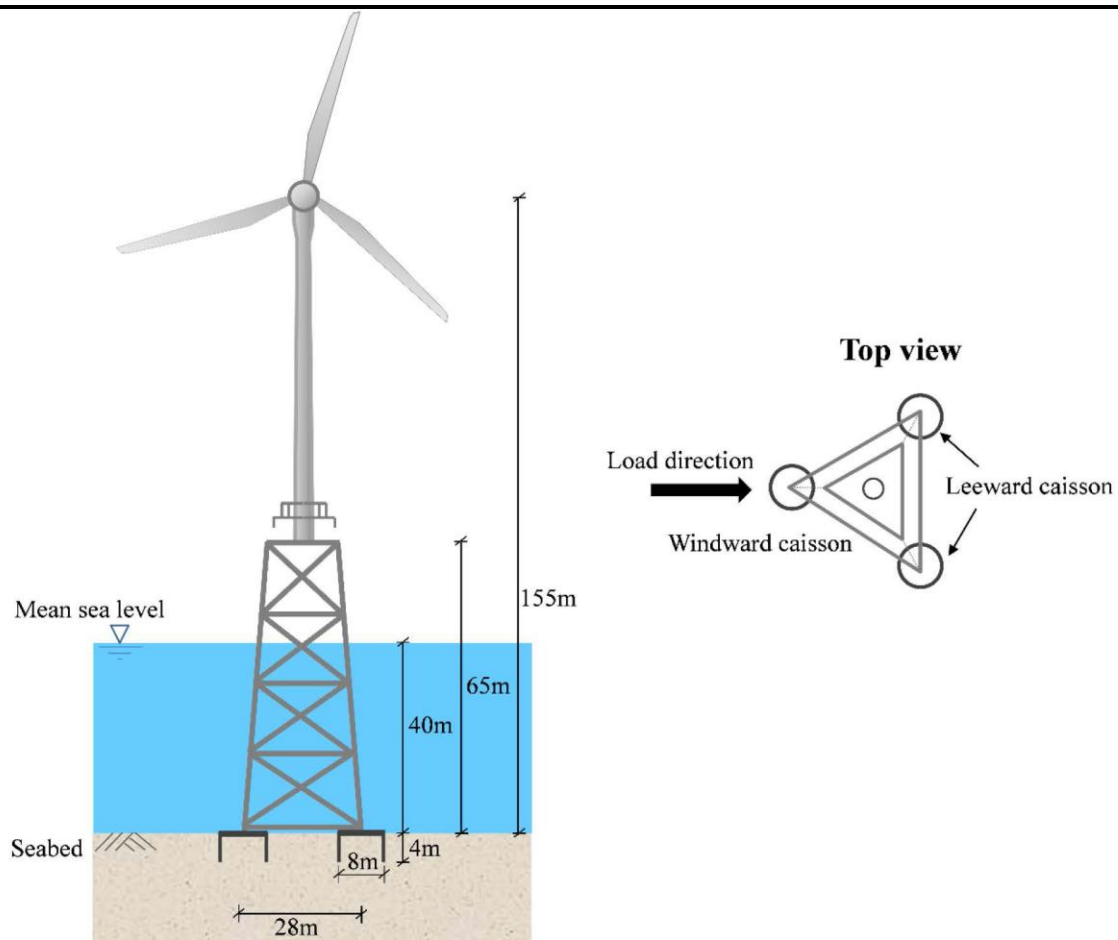


Figure 1

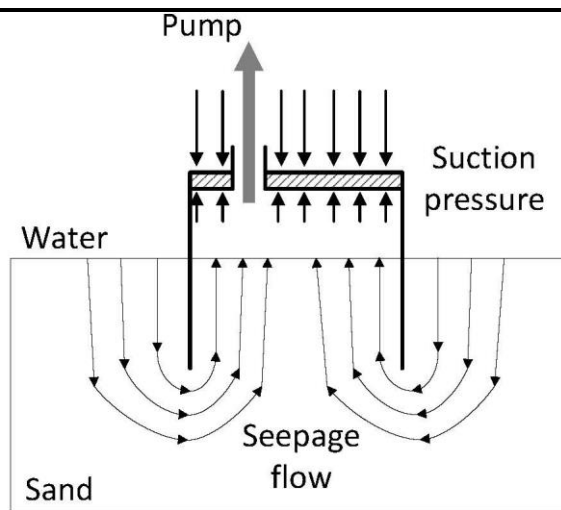


Figure 2

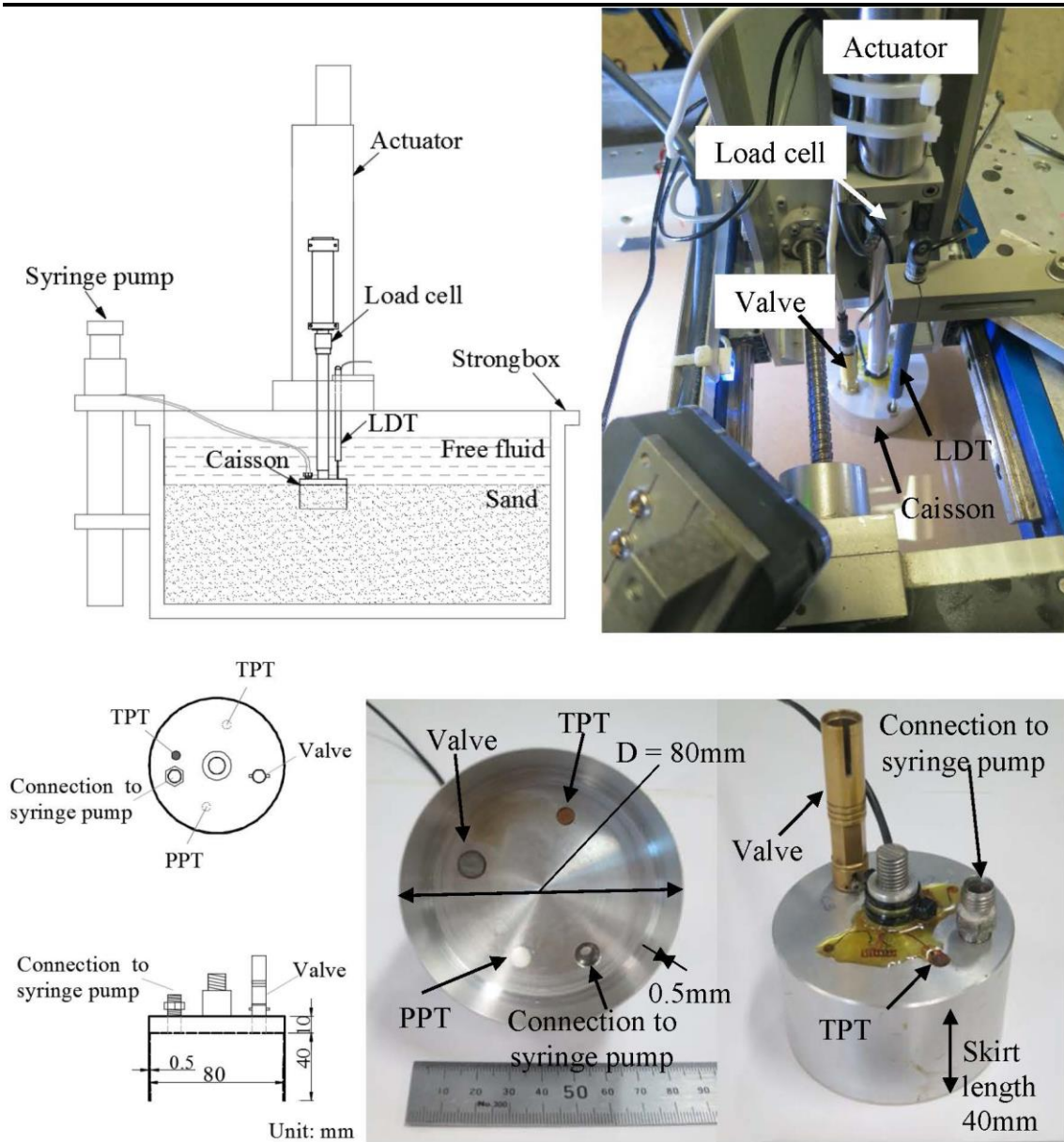


Figure 3

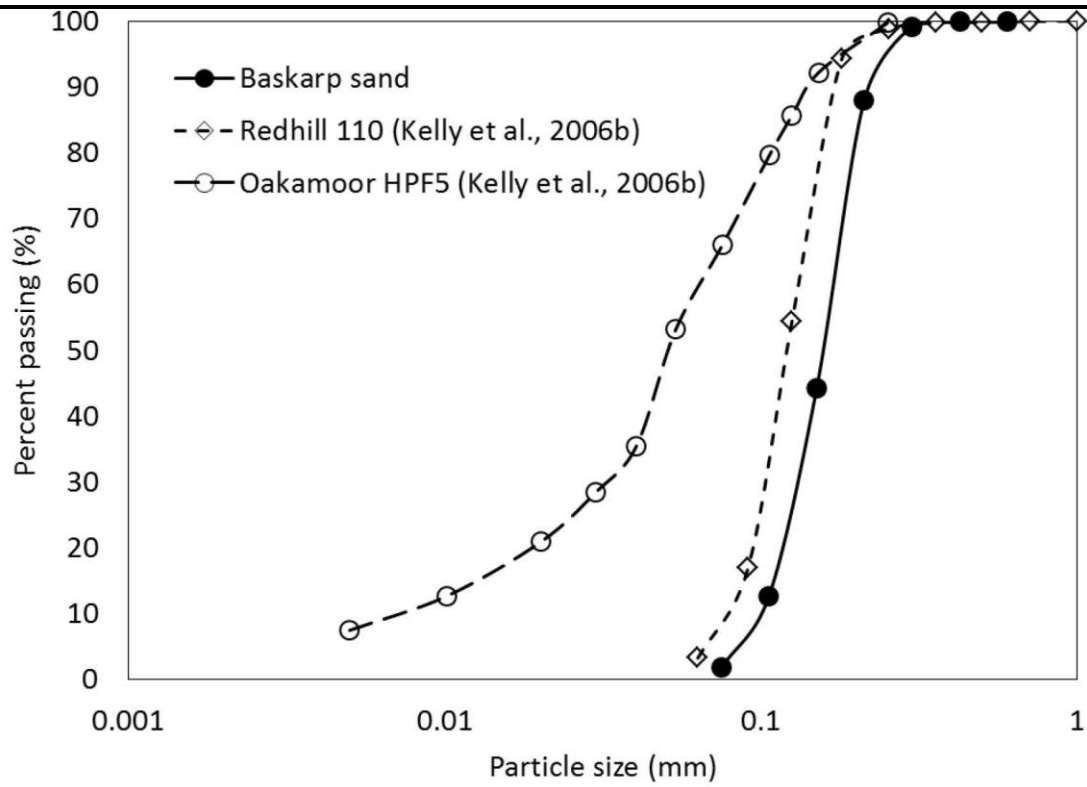


Figure 4

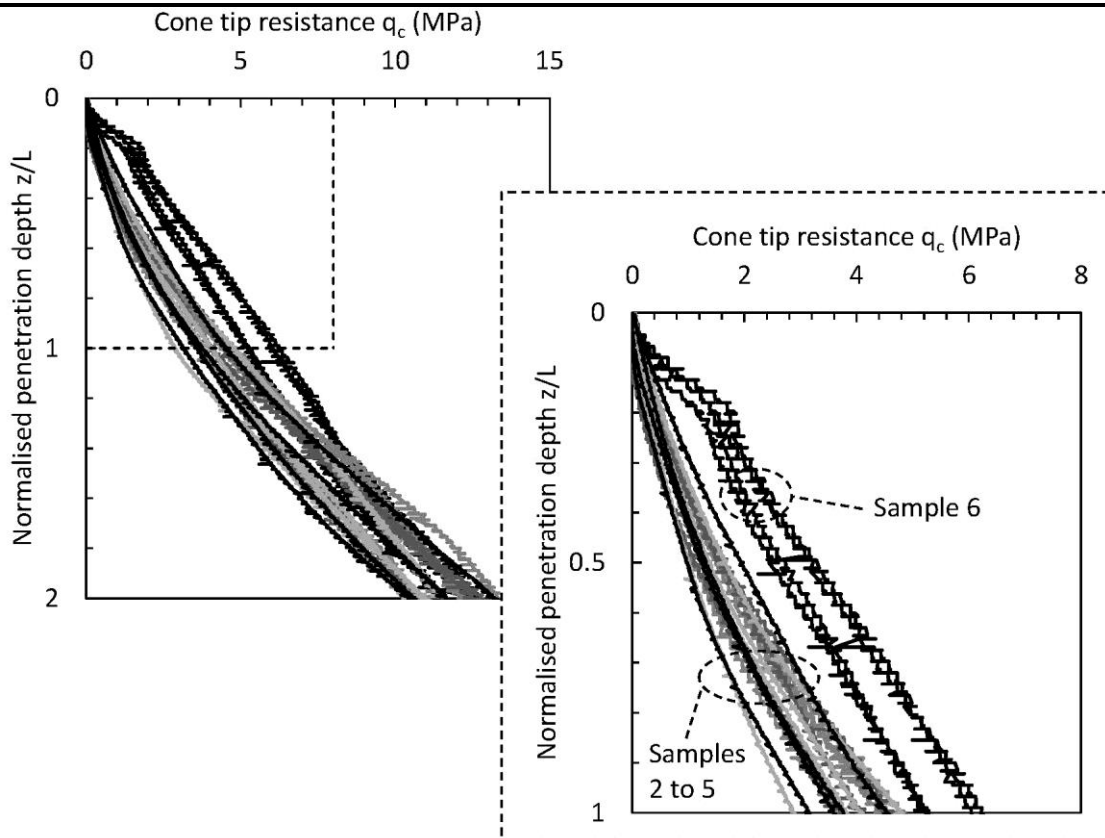


Figure 5

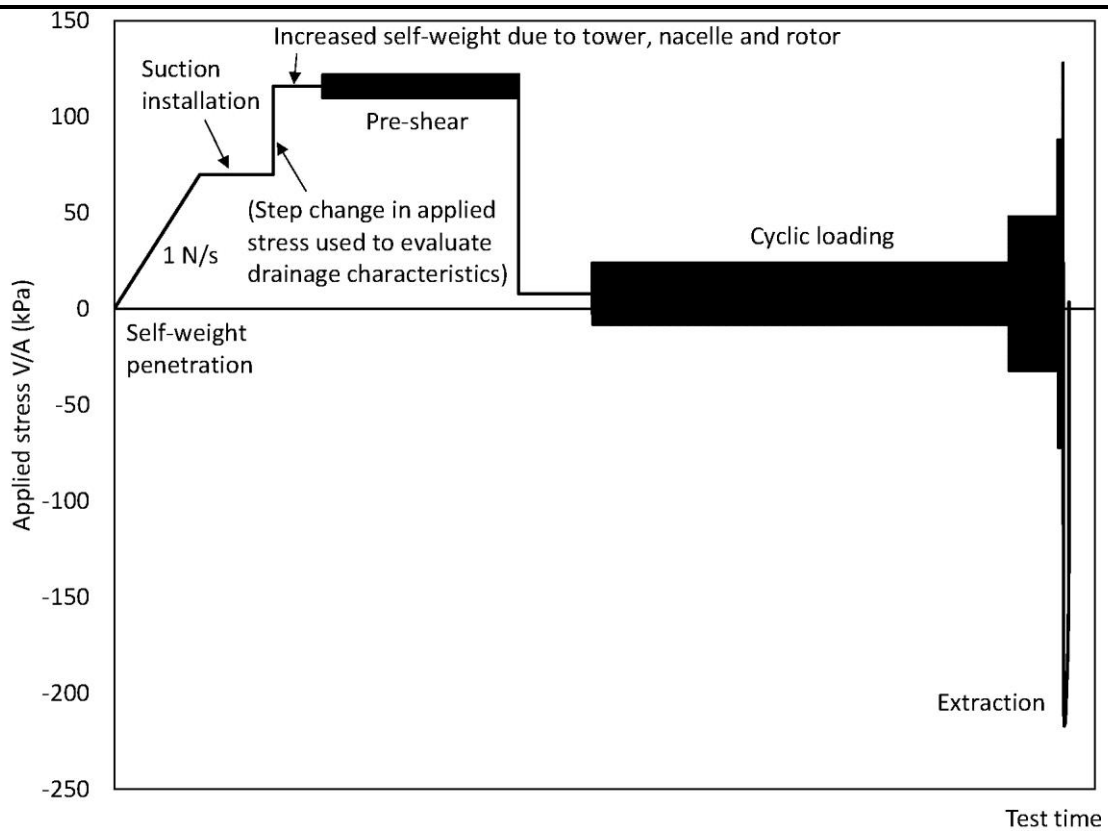


Figure 6

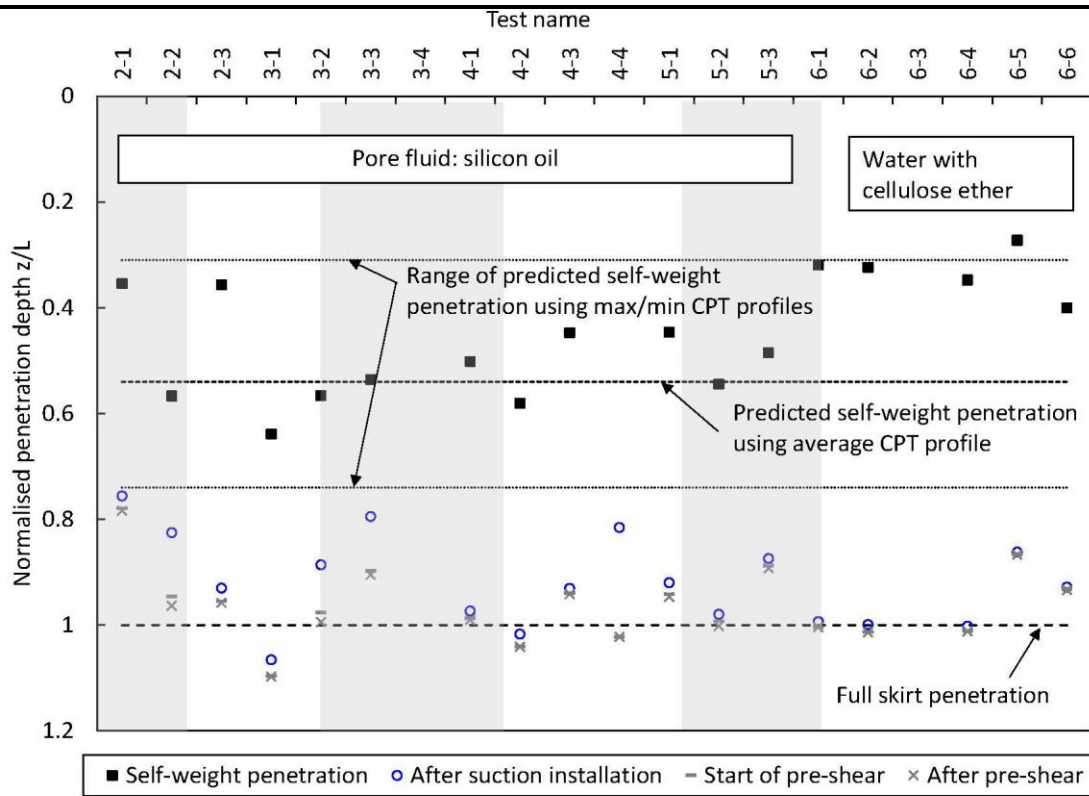
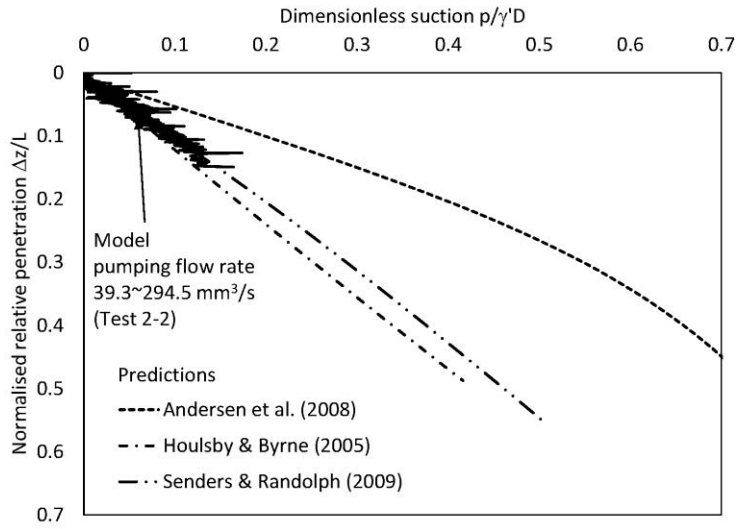
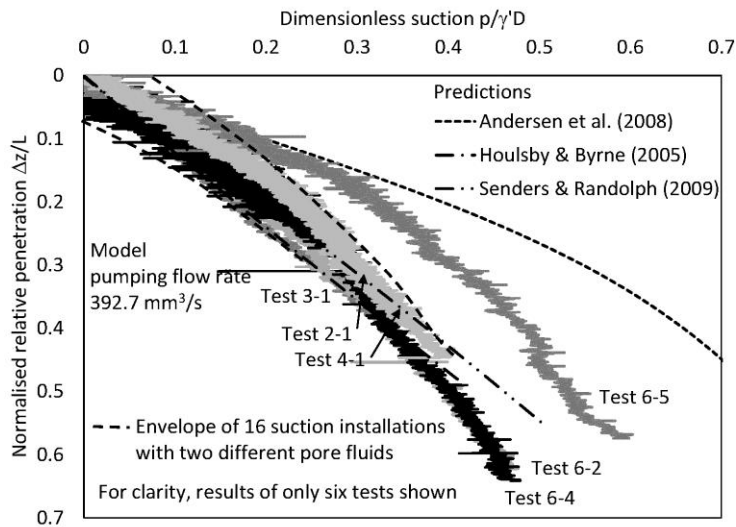


Figure 7

a)



b)



c)

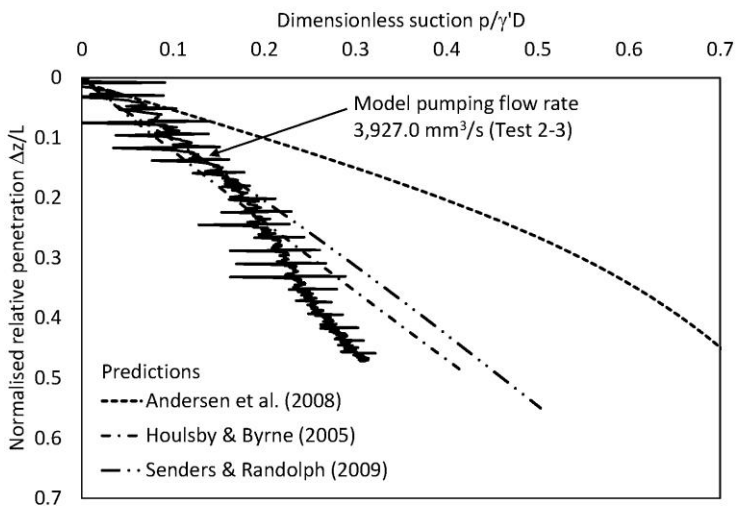
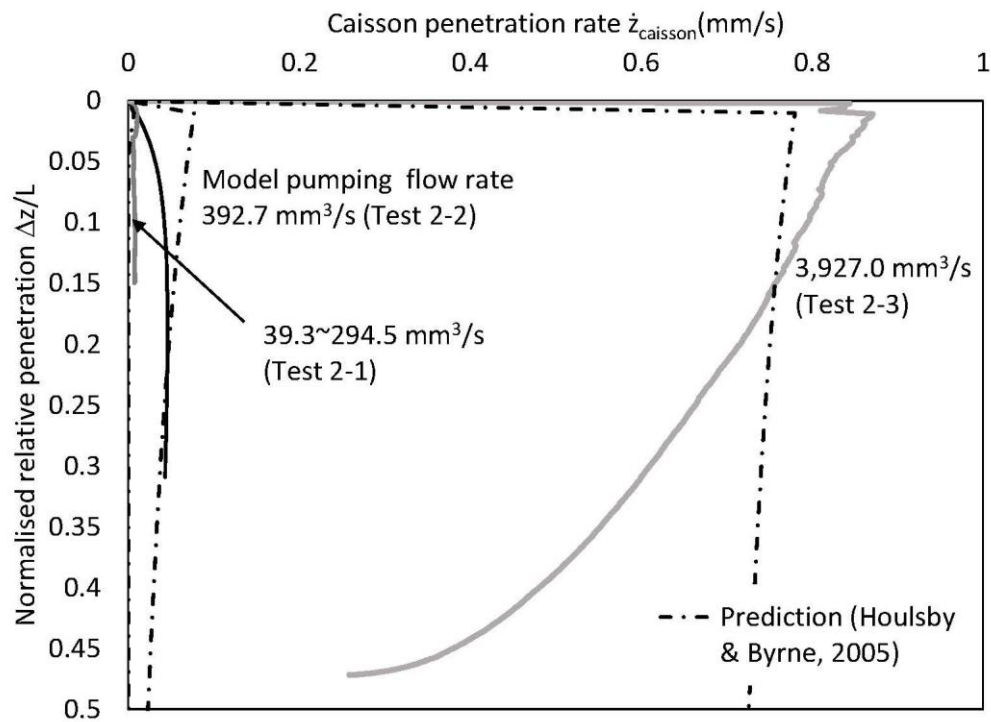


Figure_08.jpg

Accepted manuscript doi:
10.1680/jgeot.16.p.281

a)



b)

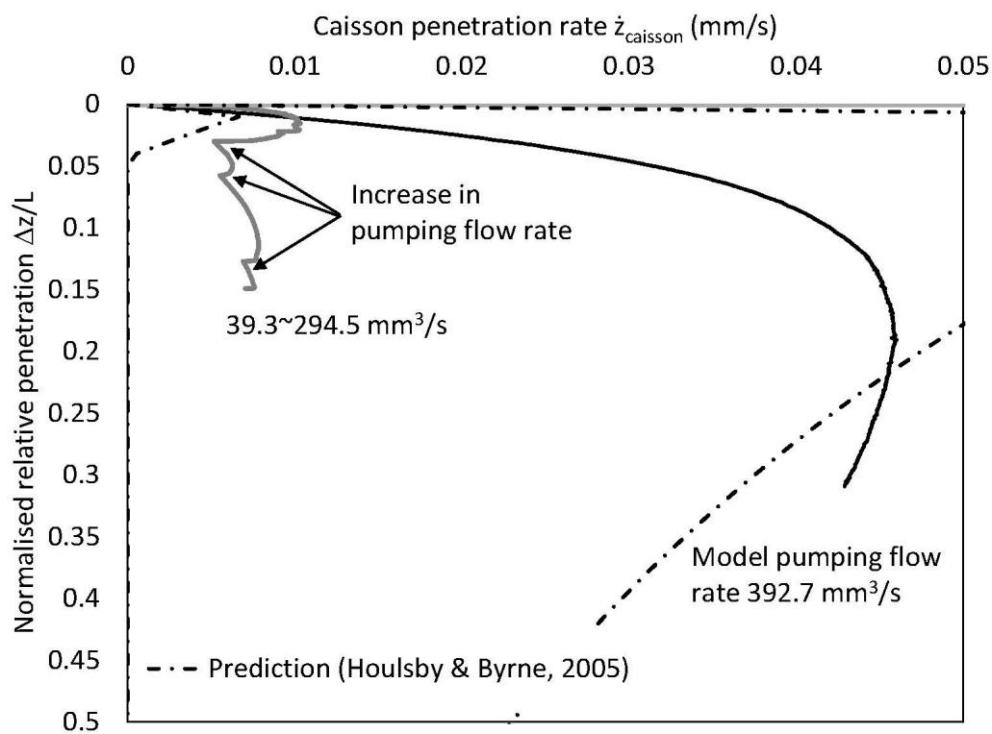


Figure 9

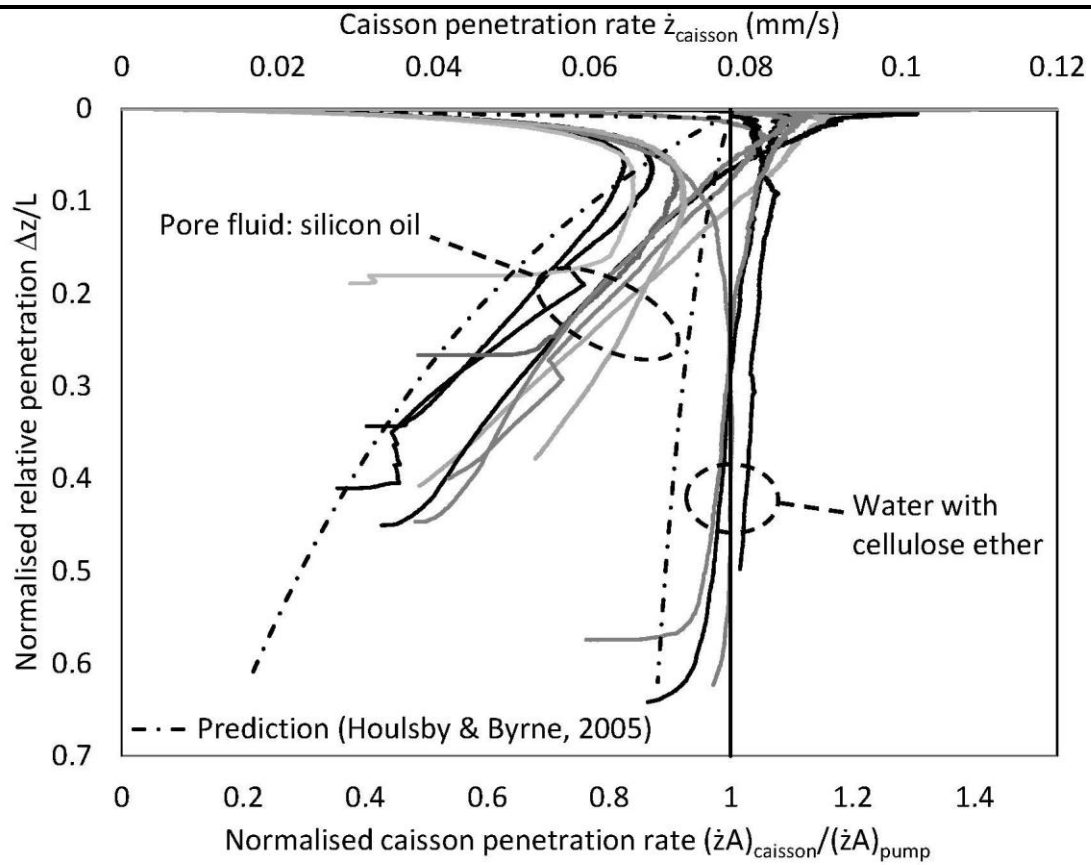


Figure 10

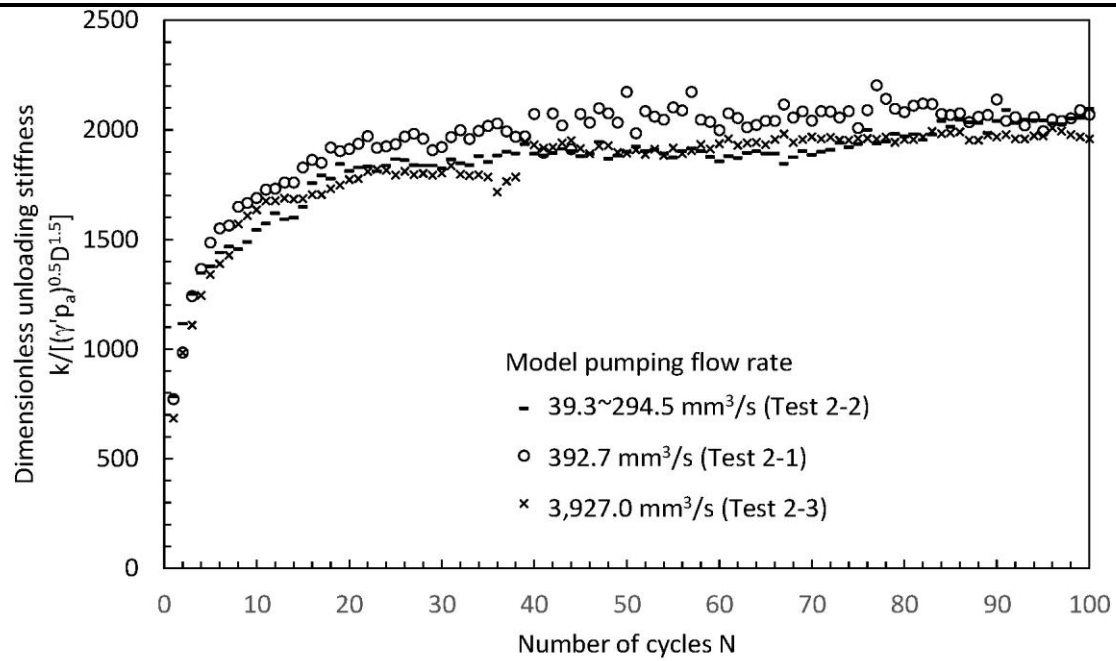


Figure 11

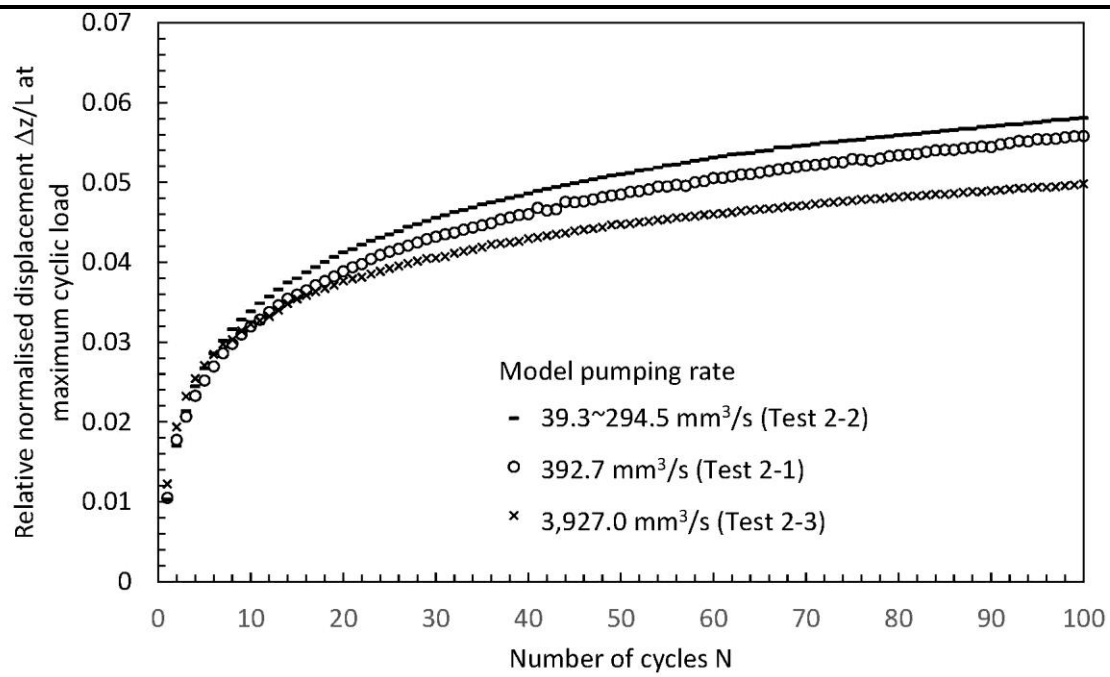


Figure 12

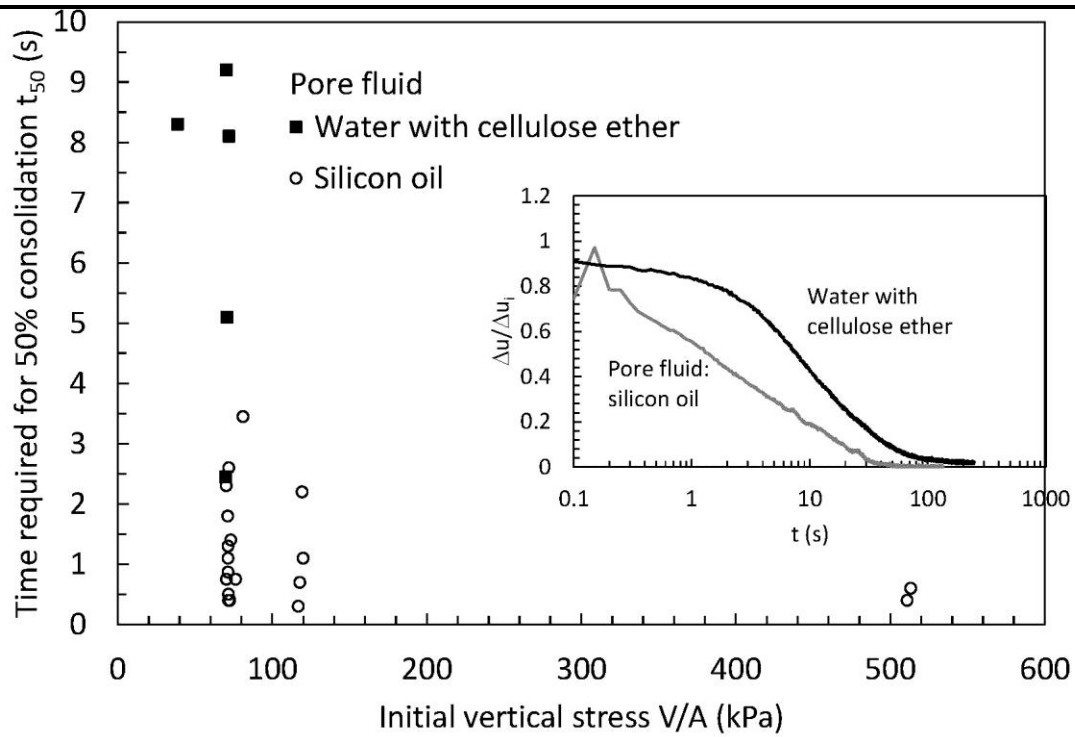
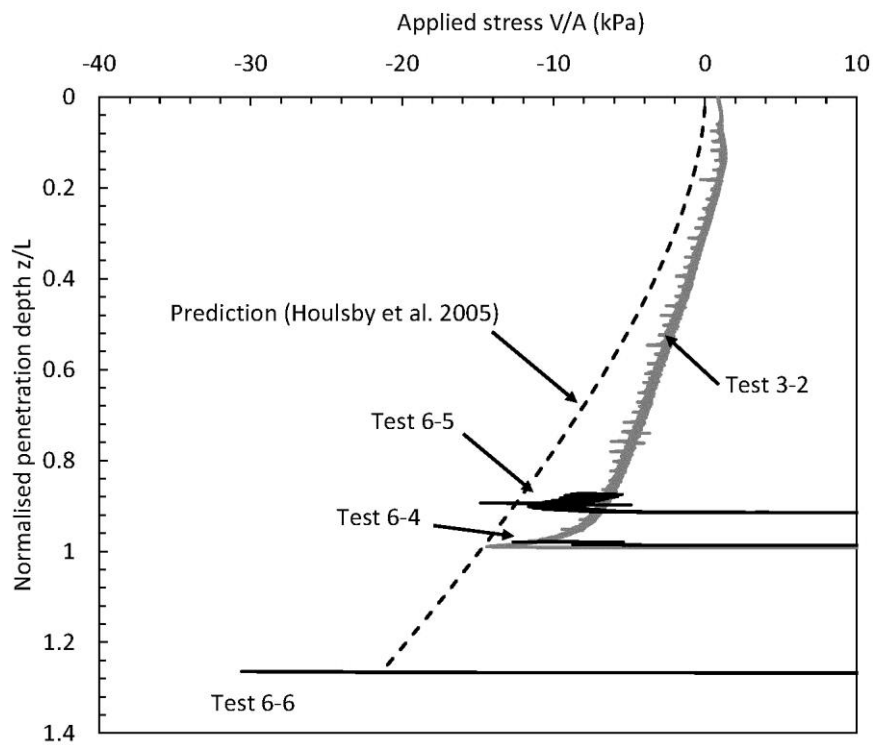


Figure 13

a)



b)

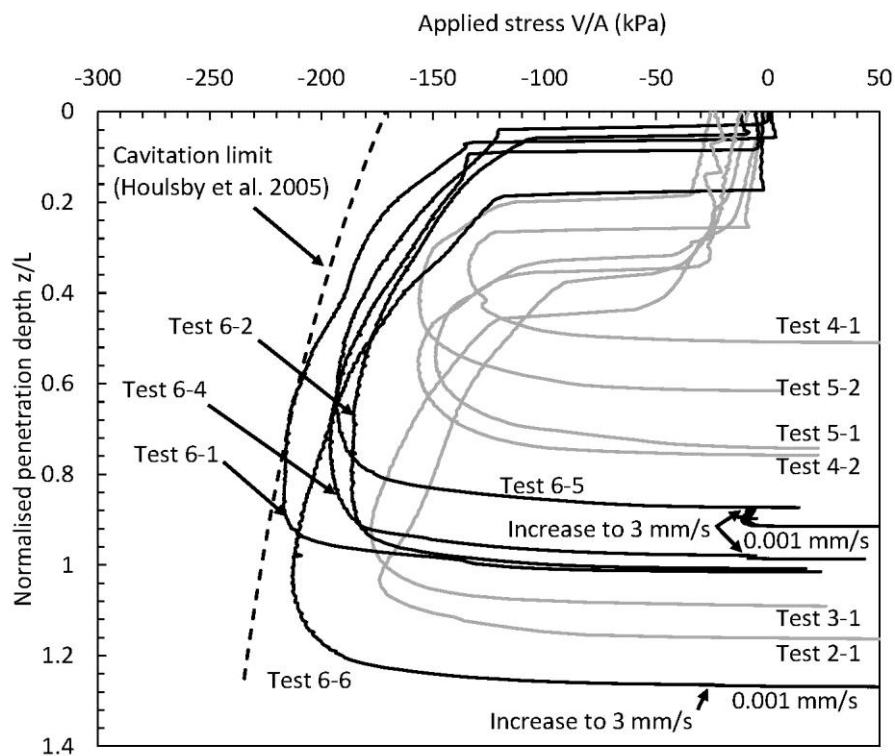


Figure 14

